

In-situ X-ray diffraction study of graphitic carbon formed during heating and cooling of amorphous C/Ni bilayers

Citation for published version (APA):

Saenger, K. L., Tsang, J. C., Bol, A. A., Chu, J. O., Grill, A., & Lavoie, C. (2010). In-situ X-ray diffraction study of graphitic carbon formed during heating and cooling of amorphous C/Ni bilayers. *Applied Physics Letters*, 96(15), 1-3. Article 153105. <https://doi.org/10.1063/1.3397985>

DOI:

[10.1063/1.3397985](https://doi.org/10.1063/1.3397985)

Document status and date:

Published: 01/01/2010

Document Version:

Publisher's PDF, also known as Version of Record (includes final page, issue and volume numbers)

Please check the document version of this publication:

- A submitted manuscript is the version of the article upon submission and before peer-review. There can be important differences between the submitted version and the official published version of record. People interested in the research are advised to contact the author for the final version of the publication, or visit the DOI to the publisher's website.
- The final author version and the galley proof are versions of the publication after peer review.
- The final published version features the final layout of the paper including the volume, issue and page numbers.

[Link to publication](#)

General rights

Copyright and moral rights for the publications made accessible in the public portal are retained by the authors and/or other copyright owners and it is a condition of accessing publications that users recognise and abide by the legal requirements associated with these rights.

- Users may download and print one copy of any publication from the public portal for the purpose of private study or research.
- You may not further distribute the material or use it for any profit-making activity or commercial gain
- You may freely distribute the URL identifying the publication in the public portal.

If the publication is distributed under the terms of Article 25fa of the Dutch Copyright Act, indicated by the "Taverne" license above, please follow below link for the End User Agreement:

www.tue.nl/taverne

Take down policy

If you believe that this document breaches copyright please contact us at:

openaccess@tue.nl

providing details and we will investigate your claim.

In situ x-ray diffraction study of graphitic carbon formed during heating and cooling of amorphous-C/Ni bilayers

K. L. Saenger, J. C. Tsang, A. A. Bol, J. O. Chu, A. Grill et al.

Citation: *Appl. Phys. Lett.* **96**, 153105 (2010); doi: 10.1063/1.3397985

View online: <http://dx.doi.org/10.1063/1.3397985>

View Table of Contents: <http://apl.aip.org/resource/1/APPLAB/v96/i15>

Published by the [American Institute of Physics](#).

Additional information on *Appl. Phys. Lett.*


Journal Homepage: <http://apl.aip.org/>

Journal Information: http://apl.aip.org/about/about_the_journal

Top downloads: http://apl.aip.org/features/most_downloaded

Information for Authors: <http://apl.aip.org/authors>

ADVERTISEMENT



Special Topic Section:
PHYSICS OF CANCER

Why cancer? Why physics? [View Articles Now](#)

In situ x-ray diffraction study of graphitic carbon formed during heating and cooling of amorphous-C/Ni bilayers

K. L. Saenger,^{a)} J. C. Tsang, A. A. Bol, J. O. Chu, A. Grill, and C. Lavoie
 IBM Semiconductor Research and Development Center Research Division, T. J. Watson Research Center,
 Yorktown Heights, New York 10598, USA

(Received 23 February 2010; accepted 28 March 2010; published online 15 April 2010)

We examine graphitization of amorphous carbon (a-C) in a-C/Ni bilayer samples having the structure Si/SiO₂/a-C(3–30 nm)/Ni(100 nm). *In situ* x-ray diffraction (XRD) measurements during heating in He at 3 °C/s to 1000 °C showed graphitic C formation beginning at temperatures T of 640–730 °C, suggesting graphitization by direct metal-induced crystallization, rather than by a dissolution/precipitation mechanism in which C is dissolved during heating and expelled from solution upon cooling. We also find that graphitic C, once formed, can be reversibly dissolved by heating to T > 950 °C, and that nongraphitic C can be volatilized by annealing in H₂-containing ambients. © 2010 American Institute of Physics. [doi:10.1063/1.3397985]

Few-layer graphene has attracted intense interest as a possible material for postsilicon electronic devices due to its high mobility, two-dimensional structure, and tunable band gap.^{1–3} Methods for forming graphene such as mechanical exfoliation from graphite³ and decomposition of single-crystal SiC (Ref. 4) are not readily scalable to the wafer-scale dimensions that are expected to be required for semiconductor manufacturing. One potentially scalable method is metal-catalyzed chemical vapor deposition (CVD), in which graphene is formed on a metallic template layer exposed to a carbon-containing gas at elevated temperature (900–1000 °C). Several groups have shown that it is possible to grow few-layer graphene on Ni and transfer it to insulating substrate layers.^{2,5,6}

We have been investigating alternative metal-catalyzed graphene formation processes utilizing solid phase sources of carbon. In this approach, the carbon is not introduced from the gas phase but rather as one of the layers in an amorphous carbon (a-C)/Ni bilayer stack. It was hoped that this approach would provide films of quality comparable to those achieved by CVD but with better control over film thickness (since the carbon supply is fixed and finite). Our own results and those of Zheng *et al.*⁷ indicate that continuous films of few-layer graphene may be produced with this approach under certain optimized conditions.

The present work focuses on the kinetics and mechanism of multilayer graphene formation in a-C/Ni bilayer structures comprising a top layer of Ni over bottom layer of a-C disposed on a thermally oxidized Si substrate. Our initial expectation was that graphene would form by a simple dissolution/precipitation mechanism in which C from the a-C layer would dissolve into the Ni layer during heating and be expelled from solution upon cooling below the solid solubility limit, the mechanism previously seen with graphene growth by CVD.^{2,5,6} However, the appearance of a surface layer of graphitic carbon after annealing at temperatures at which the C solubility in Ni is still very low (550–750 °C) suggested that a metal-induced crystallization and layer exchange mechanism analogous to that seen with Al-induced crystallization of amorphous Si (a-Si) (Refs. 8–10) might be more

likely. In this scenario, the C in Ni has a low concentration and a high transport rate. Nucleation sites for graphite (typically metal grain boundaries) provide a sink for the dissolved carbon which is replenished by continued dissolution of the a-C layer. For both the a-Si/Al and a-C/Ni cases, the driving force for crystallization is thermodynamic stability of the crystalline C or Si phase relative to the amorphous phase.

Distinguishing between these two graphitization mechanisms can be difficult without a means of determining exactly when during the thermal treatment the graphitic carbon appears. For a simple dissolution/precipitation mechanism, graphitic carbon would be expected to appear only during the cooling part of the heat treatment. For a metal-induced crystallization mechanism, graphitic carbon would be expected to appear merely after a sufficient amount of time at a sufficiently elevated temperature. In the experimental approach used here (one previously used to study metal-induced crystallization of a-Si (Ref. 11) and a-Ge (Ref. 12) as well as carbide formation¹³ in a-C/metal bilayers), *in situ* x-ray diffraction (XRD) during annealing was used to detect the formation graphitic carbon, which has a strong 002 reflection corresponding to a *d*-spacing of 0.34 nm.

Thermally oxidized substrates (SiO₂ thickness ~300 nm) were *in situ* sputter precleaned and then sequentially coated with a-C and Ni by sputter deposition from C and Ni targets in ~10 mTorr Ar. The resulting a-C/Ni bilayer samples had a-C thicknesses of 3, 10, and 30 nm and a Ni thickness of 100 nm.

In situ XRD measurements during annealing (heating and cooling at 3 °C/s to and from 1000 °C in He or N₂/H₂(5%)) were performed at the National Synchrotron Light Source of the Brookhaven National Laboratory (IBM/MIT beamline X-20C) with synchrotron radiation having a wavelength of 0.1797 nm, intensity of 10¹³ photons/s, and energy resolution of 1.5%,¹⁴ using a linear detector covering a 2θ range of ~14° centered around the 002 graphite peak. Additional *ex situ* θ–2θ XRD scans were also performed at room temperature over a wider 2θ range in a Bragg–Brentano geometry with Cu K_α radiation (λ=0.1542 nm) after rapid thermal anneals (RTAs) with 35 °C/s heating rates to 900–1000 °C in N₂ or Ar/H₂(5%), as well as after furnace anneals in N₂/H₂(5%) at 550 °C. Raman spectroscopy

^{a)}Electronic mail: saenger@us.ibm.com.

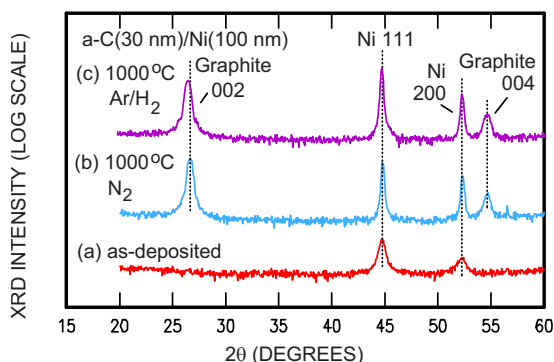


FIG. 1. (Color online) *Ex situ* XRD scans of Si/SiO₂/a-C(30 nm)/Ni(100 nm) samples before (a) and after RTA annealing at 900 °C for 1 min in (b) N₂ and (c) Ar/H₂. Note the log scale and arbitrary baseline offsets.

indicated that the graphitic carbon formed was present as a top surface layer.

Figure 1 shows *ex situ* XRD data for a-C(30 nm)/Ni(100 nm) samples before and after graphite formation induced by 900 °C/1 min RTA annealing in N₂ or Ar/H₂. Before annealing [Fig. 1(a)], 111 and 200 Ni peaks are present and graphite peaks are absent. After annealing in either ambient [Figs. 1(b) and 1(c)], strong graphite peaks appear and the Ni peaks become stronger and sharper, consistent with the Ni grain growth seen by optical microscopy.

The intensities and line shapes of the 002 graphite peak vary with the initial a-C layer thickness. As shown in Fig. 2 for the cases of 1000 °C/10 s RTA annealing in N₂ or Ar/H₂, the peak intensities are strongest for the a-C(30 nm) samples, about a factor of 10 lower for the a-C(10 nm) samples, and almost below the detection limit for the a-C(3 nm) samples. Similar results were seen for 950 °C/1 min anneals in the same ambients. The full width at half maxi-

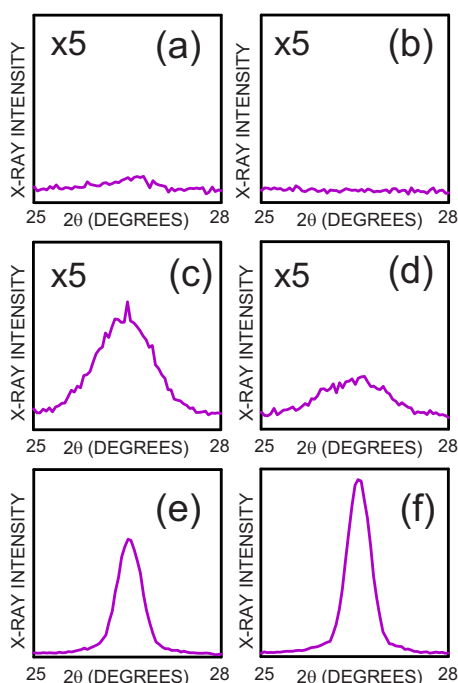


FIG. 2. (Color online) *Ex situ* XRD scans over the 002 graphite peak of Si/SiO₂/a-C/Ni(100 nm) samples with different thicknesses of a-C, after RTA annealing at 1000 °C for 10 s in ambients of N₂ or Ar/H₂: 3 nm a-C in (a) N₂ or (b) Ar/H₂; 10 nm a-C in (c) N₂ or (d) Ar/H₂; and 30 nm a-C in (e) N₂ or (f) Ar/H₂. The intensity scale is linear.

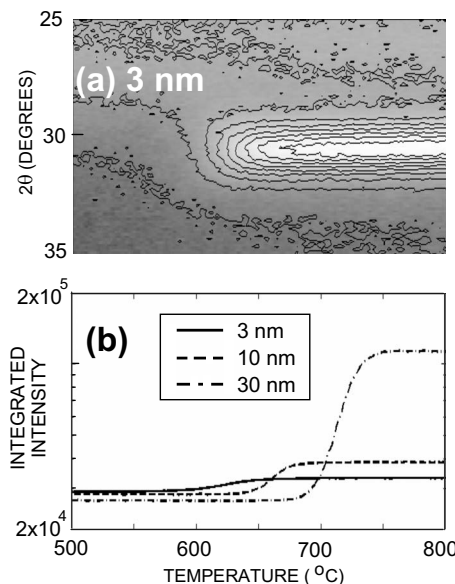


FIG. 3. *In situ* XRD results. (a) The 002 graphite peak in a Si/SiO₂/a-C(3 nm)/Ni(100 nm) sample heated in He at a ramp rate of 3 °C/s. (b) Graphite peak intensity data (integrated over the 2θ range 29.5° to 31.5°) for the same sample (line) compared to corresponding data for samples with initial a-C thicknesses of 10 nm (dashed) and (c) 30 nm (dashed-dotted). The contour lines in (a) have a linear intensity spacing.

imum values $\Delta(2\theta)$ for the a-C(10 nm) samples of Fig. 2 ($\sim 1.1^\circ$) are about twice those for the a-C(30 nm) samples. The implied crystallite sizes (computed from $\lambda/[\cos(\theta_B) \cdot \Delta(2\theta_B)]$ with the Bragg angle θ_B in radians¹⁵) are 13 nm and 32 nm, respectively, in good agreement with the initial a-C thicknesses of 10 and 30 nm.

Figure 3(a) shows a contour map of *in situ* XRD data between 500 and 800 °C for a a-C(3 nm)/Ni sample heated from room temperature to 1000 °C at 3 °C/s in He and Fig. 3(b) compares the integrated graphite intensity data for this sample with that of two others having thicker (10 and 30 nm) initial a-C layers. The graphite peak in Fig. 3(a) appears at $2\theta \sim 30.5^\circ$ during heating, lending support to a metal-induced crystallization model. Graphite formation appears to be abrupt, with “widths” of formation (defined as the difference between the minimum and maximum in the second derivative of graphite peak intensity) of about 20–30 °C. Thinner a-C layers were observed to have both an earlier mean temperature of graphite formation (defined as the temperature at which the first derivative of the graphite peak intensity is a maximum), with values of $\sim 640^\circ\text{C}$ for 3 nm, 680°C for 10 nm, and 730°C for 30 nm, as well as an earlier onset of graphite formation. The latter result was counterintuitive in that we expected the onset temperature to be independent of a-C layer thickness. We speculate that these differences may be due to interface energy effects or to the influence of interfacial or incorporated C on the time evolution of the Ni grain structure. For example, very thin a-C layers may be inherently more unstable, or some rate-limiting diffusion process necessary for Ni grain growth may be faster at SiO₂/Ni interfaces which might form (at least in localized regions) at an earlier stage of heating with thinner (and more easily consumed) a-C layers. However, it should be noted that the 3 nm a-C samples showed more variability, with some showing no detectable graphite XRD intensity at all.

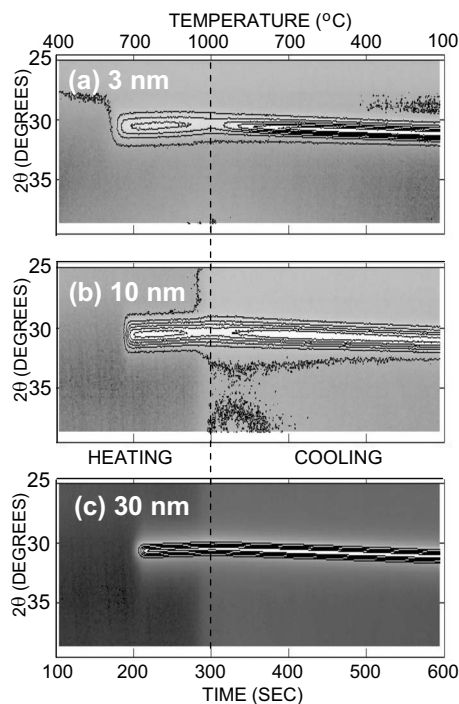


FIG. 4. Contour maps of *in situ* XRD results showing the 002 graphite peak in Si/SiO₂/a-C/Ni(100 nm) samples heated to and cooled from 1000 °C in He at a ramp rate of 3 °C/s for a-C thicknesses of (a) 3 nm, (b) 10 nm, and (c) 30 nm. The contour lines have a linear intensity spacing that is different for each a-C thickness.

Figure 4 shows contour maps of *in situ* XRD data for the same samples as a function of time during heating to and cooling from 1000 °C at 3 °C/s. All three samples show a decrease in graphite intensity during heating from ~950 to 1000 °C, and an increase in graphite intensity during cooling from 1000 to ~950 °C. This clearly indicates that the graphite formed during heating can also undergo a reversible dissolution/precipitation as the sample is thermally cycled. This effect is most pronounced for the thinnest a-C sample, as one might expect; while the amount of reversibly dissolved C is limited by the solubility of C in Ni and thus the same for all three a-C thicknesses, this dissolved a-C is a much larger fraction of the total amount of carbon for the thinner a-C samples.

In both the 3 and 10 nm a-C samples of Fig. 4, the graphite peak intensities reached during cooling are stronger than those seen during heating. Various factors might account for this, including (i) continued precipitation of dissolved carbon and/or (ii) changes in sample morphology and/or detection geometry resulting in the same amount of graphitic carbon having a stronger XRD signal. All three samples show shifts in 2θ peak position during heating and cooling, reflecting a thermal expansion/contraction of the lattice d -spacings (proportional to $(\sin \theta_B)^{-1}$) that is in close agreement with literature values for the graphite out-of-plane thermal expansion coefficient (~ 25 ppm/°C).

Given the similarity of the *ex situ* XRD results for N₂ and Ar/H₂ RTA treatments at 950–1000 °C, we were surprised at the absence of graphite in the *in situ* XRD signals from the 10 and 30 nm a-C samples annealed in ambients of N₂/H₂. We suspect that nongraphitic carbon is lost through

formation of volatile hydrocarbons produced by carbon + hydrogen reactions when ramp rates are slow (3 °C/s), an explanation that is supported by additional *ex situ* XRD measurements. For 30 nm a-C samples, we found that 550 °C/2 h furnace annealing in N₂/H₂ produced no graphite signal, whereas the same anneal in N₂ produced graphite intensities about a third of those found for RTA anneals of a fresh sample at 900–1000 °C. In addition, RTA treatments of 900 °C/1 min in N₂ produced no graphite in samples previously given the N₂/H₂ 550 °C/2 h anneal. It was also found that 550 °C/2 h anneals in N₂/H₂ performed subsequent to formation of graphitic carbon by 900 °C/1 min N₂ annealing had no effect on the graphite peak intensity, supporting the notion that the C removed by the H₂ is amorphous rather than graphitic.

In summary, we have used *in situ* XRD during annealing to examine the formation of graphitic carbon from a-C/Ni bilayers. It was found that a simple dissolution/precipitation mechanism cannot account for our observation that graphitic carbon is first formed during heating rather than cooling. While a dissolution/precipitation mechanism is present, it is seen only after graphitic carbon has already formed; the initial formation mechanism appears to be a metal-induced crystallization and layer exchange mechanism analogous to that seen with Al-induced crystallization of a-Si. It was also observed that low temperature annealing in H₂-containing ambients can volatilize nongraphitic carbon.

This work was supported by DARPA under Contract No. FA8650-08-C-7838 through the CERA program. We thank C.-Y. Sung for management support, the Microelectronics Research Laboratory staff for their contributions to sample preparation, and J. Jordan Sweet for help with the synchrotron XRD experiments (supported under DOE Contract No. DE-AC02-98CH-10886).

- ¹A. K. Geim and K. S. Novoselov, *Nature Mater.* **6**, 183 (2007).
- ²K. S. Kim, Y. Zhao, H. Jang, S. Y. Lee, J. M. Kim, K. S. Kim, J.-H. Ahn, P. Kim, J.-Y. Choi, and B. H. Hong, *Nature (London)* **457**, 706 (2009).
- ³K. S. Novoselov, A. K. Geim, S. V. Morozov, D. Jiang, Y. Zhang, S. V. Dubonos, I. V. Grigorieva, and A. A. Firsov, *Science* **306**, 666 (2004).
- ⁴C. Berger, Z. Song, T. Li, X. Li, A. Y. Ogbazghi, R. Feng, Z. Dai, A. N. Marchenkov, E. H. Conrad, P. N. First, and W. A. de Heer, *J. Phys. Chem. B* **108**, 19912 (2004).
- ⁵Q. Yu, J. Lian, S. Siriponglert, H. Li, Y. P. Chen, and S.-S. Pei, *Appl. Phys. Lett.* **93**, 113103 (2008).
- ⁶A. Reina, X. Jia, J. Ho, D. Nezich, H. Son, V. Bulovic, M. S. Dresselhaus, and J. Kong, *Nano Lett.* **9**, 30 (2009).
- ⁷M. Zheng, K. Takei, B. Hsia, H. Fang, X. Zhang, N. Ferralis, H. Ko, Y.-L. Chueh, Y. Zhang, R. Maboudian, and A. Javey, *Appl. Phys. Lett.* **96**, 063110 (2010).
- ⁸O. Nast and S. R. Wenham, *J. Appl. Phys.* **88**, 124 (2000).
- ⁹O. Nast and A. J. Hartmann, *J. Appl. Phys.* **88**, 716 (2000).
- ¹⁰P. I. Widenborg and A. G. Aberle, *J. Cryst. Growth* **242**, 270 (2002).
- ¹¹W. Knaepen, C. Detavernier, R. L. Van Meirhaeghe, J. Jordan Sweet, and C. Lavoie, *Thin Solid Films* **516**, 4946 (2008).
- ¹²W. Knaepen, S. Gaudet, C. Detavernier, R. L. Van Meirhaeghe, J. Jordan Sweet, and C. Lavoie, *J. Appl. Phys.* **105**, 083532 (2009).
- ¹³W. P. Leroy, C. Detavernier, R. L. Van Meirhaeghe, and C. Lavoie, *J. Appl. Phys.* **101**, 053714 (2007).
- ¹⁴G. B. Stephenson, K. F. Ludwig, Jr., J. L. Jordan-Sweet, S. Brauer, J. Mainville, Y. S. Yang, and M. Sutton, *Rev. Sci. Instrum.* **60**, 1537 (1989).
- ¹⁵S. Mader, in *Handbook of Thin Film Technology*, edited by L. I. Maissel and R. Glang (McGraw-Hill, New York, 1970), Chap. 9, p. 8.